

Electron impact total ionization cross sections of beryllium and boron isoelectronic ions

M.R. Talukder

Received: 31 May 2008 / Revised version: 25 June 2008 / Published online: 3 October 2008
© Springer-Verlag 2008

Abstract A simple user-friendly empirical formula is proposed to calculate the electron impact total single ionization cross sections of beryllium-like Be, B⁺, C²⁺, N³⁺, O⁴⁺, Ne⁶⁺, Fe²²⁺, Hg⁷⁶⁺, and U⁸⁸⁺ and boron-like B, C⁺, N²⁺, O³⁺, Ne⁵⁺, Fe²¹⁺, Kr³¹⁺, and Xe⁴⁹⁺ targets. A simplified and modified version of the Bell formula is used in the present model incorporating the ionic correction factor. The predicted ionization cross sections are compared with the available experimental and theoretical results. Excellent agreements are found for the incident energies ranging from threshold to 10⁶ eV considered herein. The presented results achieve a level of agreement that is better than the calculations from the existing theoretical methods and empirical models. Hence, this model may be an excellent choice, due to its simplicity, for the practitioners in the fields of applied sciences and technologies.

PACS 34.80.Dp · 34.80.Pj

1 Introduction

Electron impact (EI) plays an important role for the understanding of atomic structure and collision mechanisms. In particular, electron impact ionization (EII) cross sections are widely used in modeling the structure and dynamics of plasmas [1, 2], e.g. in the modeling of low- and high-temperature plasmas and laser–plasma interactions. Besides, the knowledge of ionization cross sections has wide applications in

radiation physics, mass spectrometry, astrophysics, materials research, and so on.

In recent years, various quantum methods have been proposed [3–14] to calculate EI total single ionization (EITI) cross sections, by solving the Schrödinger equation, for different atomic and ionic targets. However, they are confined to simple atomic and ionic targets only. Although these rigorous calculations are arduous, the performance of these methods in describing experimental data is rather limited. The distorted wave Born approximation with exchange (DWBX [5]), distorted wave Born approximation with R-matrix (DWBARM [6]), no-exchange distorted wave Coulomb–Born approximation (NXDCB [7]), orthogonalized Born–Oppenheimer approximation (OBO [8]), and relativistic distorted wave Born approximation (RDWBA [9]) models are employed to calculate cross sections. However, experiments and quantum calculations provide cross sections for discrete energies and selected species. These models require large computation time and, moreover, do not generate user-friendly cross sections for the practitioners in the field of applied sciences. Therefore, the requirement can be best fulfilled by analytic models, which can provide reliable data over wide domains of validity.

Several classical and empirical models are reviewed [15] and proposed [16–32]. A semi-classical model, formulated by Gryzinski [16], calculates inaccurate cross sections in most cases and valid for few atoms and ions. Kim et al. [17, 18] proposed a binary encounter Bethe (BEB) model for direct EI ionization cross sections, and scaled Born cross sections for the dominant inner-shell excitation–autoionization, only for C, N, and O atoms. This model calculates cross sections from threshold to a few keV only. On the other hand, the Deutsch–Märk (DM) (Deutsch et al. [19–21]), Bernshtam et al. (henceforth, referred to as the BRY [27])

M.R. Talukder (✉)
Department of Applied Physics & Electronic Engineering,
University of Rajshahi, Rajshahi 6205, Bangladesh
e-mail: mrtalukder@ru.ac.bd

model), and Lotz empirical formulae [28, 29] are extensively used to calculate and represent cross sections for atoms and ions. A simple empirical BRY model is valid for few selected ionic targets with charge $q > 1$. Godunov and Ivanov [30] proposed a number of empirical models for calculating cross sections without generalization of model parameters. However, a user-friendly model capable of calculating sufficiently accurate EITI cross sections for a variety of species with a wide range of energies may contribute to fill up, to some extent, the gap between the available cross section data and the demand level. With this motivation, we propose a simple modification of Bell et al. [31], referred to as the BELI model [30], to improve the efficiency and to reduce the number of fitting coefficients. In the present work, it is our intension to explore the efficiency of the BELI model to beryllium and boron isoelectronic ions introducing a simple ionic correction factor as a multiplier. The model so framed is, hereafter, referred to as the MSBELL model. The MSBELL model is applied to calculate EITI cross sections for the beryllium- and boron-like targets from threshold to 10^6 eV. Comparisons are made with the available experimental data and other theoretical calculations.

In Sect. 2, we present a brief description of the MSBELL model. A discussion of the results is furnished in Sect. 3 and a brief summary of the conclusions is drawn in Sect. 4.

2 Outline of the model

A simple semi-empirical model [31] is proposed for the description of the EITI cross sections of atoms and ions. The (BELI) model is given [30] as

$$\sigma_{\text{BELI}}(E) = \frac{1}{EI} \left\{ A \ln(E/I) + \sum_{k=1}^5 B_k (1 - I/E)^k \right\}. \tag{1}$$

Here, I is the ionization potential, E is the kinetic energy of the incident electrons, and A and B_k are the fitting coefficients.

We propose an empirical model by simplifying and modifying the BELI formula, henceforth referred to as the SBELL model, to explore the efficiency, for the description of EITI cross sections of ionic targets. The EITI cross section σ_{SBELL} is given by

$$\sigma_{\text{SBELL}}(E) = \sum_{nl} \frac{N_{nl} I_{nl}}{E} \{ A_{nl} \ln(E/I_{nl}) + B_{nl} (1 - I_{nl}/E) \}, \tag{2}$$

where I_{nl} is the ionization potential of the ionizing nl orbit. A_{nl} and B_{nl} are the fitting coefficients and are expressed as a function of the normalized potential U_R . E and I_{nl} both expressed in eV. N_{nl} is the number of electrons in the ionizing

nl orbit. The parameter A_{nl} represents the Bethe coefficient and determines the high-energy behavior of the cross section. Here, the summation is over the orbital nl of the target. Equation (2) contains two orbital-dependent coefficients A_{nl} and B_{nl} . The factor $N_{nl} I_{nl}/E$ in (2) is introduced, instead of $1/EI$ in (1), in line with the empirical model of Kim and Rudd [17]. This model also ensures the appropriate nature of the cross sections at both low and high impact energies. However, we propose further modification in (1) by introducing the ionic correction factor for the ionic targets. As is well known, the ionic effect decreases with the increase of incident electron energy. In light of this fact, we suggest an ionic correction [33] in the form of a multiplying factor F_I :

$$F_I = 1 + m \left(\frac{q}{ZU_R} \right)^\lambda, \tag{3}$$

where m and λ are the fitting parameters. The optimum values obtained for m and λ , as will be discussed later, are 1.5 and 0.5, respectively.

The proposed MSBELL model finally takes the following form for the description of EITI cross sections σ_{MSBELL} as

$$\sigma_{\text{MSBELL}} = F_I \sigma_{\text{SBELL}}(E). \tag{4}$$

Hence, in (4) the fitting coefficients A_{nl} and B_{nl} are generalized by making them dependent on I_{nl} . The coefficients A_{nl} and B_{nl} are expressed as follows.

For Be-like ions: (a) for $2s$ orbital (i) for $1 \leq U_R \leq 100$

$$A_{nl} = \frac{1.64 \times 10^{-10} U_R}{(1 + 77U_R)^{3.1}}, \tag{5a}$$

$$B_{nl} = -\frac{3.46 \times 10^{-11} U_R}{(1 + 69U_R)^{3.1}}, \tag{5b}$$

(ii) for $100 \leq U_R \leq 10^4$

$$A_{nl} = \frac{2.76 \times 10^{-10} U_R}{(1 + 89.65U_R)^{3.1}}, \tag{5c}$$

$$B_{nl} = -\frac{8.91 \times 10^{-12} U_R}{(1 + 69U_R)^{2.9}}, \tag{5d}$$

(b) for $1s$ orbital (i) for $1 \leq U_R \leq 100$

$$A_{nl} = \frac{1.10 \times 10^{-10} U_R}{(1 + 89.65U_R)^{3.1}}, \tag{5e}$$

$$B_{nl} = -\frac{2.85 \times 10^{-11} U_R}{(1 + 69U_R)^{3.1}}, \tag{5f}$$

(ii) for $100 \leq U_R \leq 10^4$

$$A_{nl} = \frac{2.56 \times 10^{-10} U_R}{(1 + 89.65U_R)^{3.1}}, \tag{5g}$$

$$B_{nl} = -\frac{5.33 \times 10^{-11} U_R}{(1 + 69U_R)^{3.1}}. \quad (5h)$$

On the other hand, for B-like ions: (c) for $2p$ orbital (i) for $1 \leq U_R \leq 100$

$$A_{nl} = \frac{2.44 \times 10^{-11} U_R}{(1 + 69U_R)^{2.68}}, \quad (6a)$$

$$B_{nl} = -\frac{5.24 \times 10^{-13} U_R}{(1 + 69U_R)^{2.3}}, \quad (6b)$$

(ii) $1s$ and $2s$ orbitals

$$A_{nl} = \frac{5.20 \times 10^{-10} U_R}{(1 + 69U_R)^{3.39}}, \quad (6c)$$

$$B_{nl} = -\frac{9.60 \times 10^{-11} U_R}{(1 + 69U_R)^{3.05}}, \quad (6d)$$

(d) for $2p$ orbital (i) for $100 \leq U_R \leq 10^4$

$$A_{nl} = \frac{1.49 \times 10^{-12} U_R}{(1 + 89.65U_R)^{2.55}}, \quad (6e)$$

$$B_{nl} = -\frac{9.81 \times 10^{-12} U_R}{(1 + 69U_R)^{2.95}}, \quad (6f)$$

(ii) $1s$ and $2s$ orbitals

$$A_{nl} = \frac{2.32 \times 10^{-8} U_R}{(1 + 69U_R)^{3.6}}, \quad (6g)$$

$$B_{nl} = -\frac{2.56 \times 10^{-10} U_R}{(1 + 69U_R)^{3.1}}. \quad (6h)$$

The ionization potential is normalized by $U_R = I_{nl}/R$, where R is the Rydberg energy. The units of A_{nl} and B_{nl} are expressed in cm^2 . For the heavier ions, one has to take the relativistic effect into account in (4), but it is not necessary because the fitting parameters are obtained with account for the experimental cross sections in the considered energy range and provide accuracy within the experimental error.

3 Results and discussion

The ionization potentials I_{nl} have been collected from the published results [34] for the neutral targets, and calculated using Dirac–Hartree–Fock code [35] for the ionic targets. EITI cross sections are calculated by applying the proposed MSBELL model for the beryllium and boron isoelectronic systems, using (4) along with (5) and (6), respectively, taking into account the incident electron energies from threshold to 10^6 eV. The results are presented for Be-like Be, B^{1+} , C^{2+} , N^{3+} , O^{4+} , Ne^{6+} , Fe^{22+} , Hg^{76+} , and U^{88+} targets and for B-like B, C^{1+} , N^{2+} , O^{3+} , Ne^{5+} , Fe^{21+} , Kr^{31+} ,

and Xe^{49+} targets. Most recent experimental as well as theoretical results are taken into consideration for comparison with the results obtained by the MSBELL model.

The parameter values $m = 1.5$ and $\lambda = 0.5$ for the ionic correction factor F_I in (3) are optimized in such a way that (4) describes the best EITI cross sections with respect to the experimental data for the studied range of incident energies and for the targets considered herein. The coefficients of the parameters A_{nl} and B_{nl} in (5) and (6) are determined from the overall best fit of the MSBELL predicted cross sections to the experimental data. A measure of the quality of best fit is determined by minimizing chi-square defined as

$$\chi^2 = \sum_i \left[\frac{\sigma_t(E_i) - \sigma_x(E_i)}{\sigma_x(E_i)} \right]^2,$$

where $\sigma_t(E_i)$ and $\sigma_x(E_i)$ refer, respectively, to the theoretical and experimental cross sections at the energy point E_i . The optimum values of the coefficients, in terms of which the parameters A_{nl} and B_{nl} are defined, are obtained using a non-linear least-square fitting program.

The open and filled symbols are used in the figures to represent, respectively, the quantum and experimental results. The continuous and dashed lines are used, respectively, to represent the cross sections calculated by the MSBELL model and by the other classical, semi-classical, or empirical models.

The EITI cross sections of beryllium-like B^+ , C^{2+} , and N^{3+} ions are shown in Fig. 1a–c, respectively. The MSBELL predictions for B^+ are displayed in Fig. 1a, along with the experimental cross sections [36] and the results of DWBX [37], the binary encounter dipole model with relativistic and ionic corrections (RQIBED [22]), and the BRY [27] theories. The DWBX and RQIBED results agree well with the experimental results but the BRY results largely underestimate the experimental results over the whole studied energy region. The experimental results [36] indicate that the enhancement in cross sections comes from the contributions of metastable states. Besides, the contributions from the excitation–autoionization (EA) process may be accountable for this enhancement. However, good agreements are found between the MSBELL and experimental cross sections over the considered range of incident energies.

In Fig. 1b, we present the MSBELL cross sections for C^{2+} , along with the experimental results [36, 38, 39], and findings from the distorted wave Coulomb–Born approximation with exchange (DCBX [41]), NXDCB [7], DWBX [37], BRY [27], and RQIBED [22] theories. The experimental results [36] suggest that 40% contributions in cross sections originate from the metastable state with a mixture of the 60% and 40% contributions from the ground and metastable states, respectively. Similar to the B^+ target, the BRY calculations are reduced in magnitude. The RQIBED

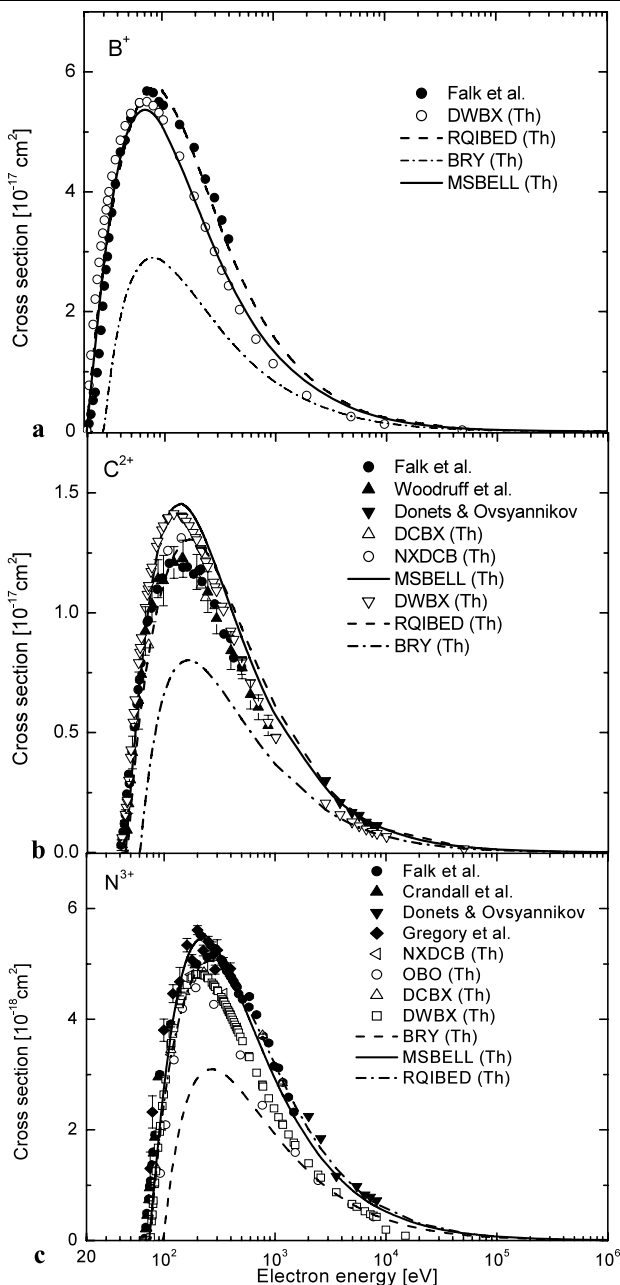


Fig. 1 Electron impact total ionization cross sections for Be-like ions: (a) B^+ , (b) C^{2+} , and (c) N^{3+}

cross sections shift in peak position towards the higher energies relative to the experimental results. Nevertheless, the MSBELL prediction agrees well with the DWBX, DCBX, and the experimental data except in the peak region.

The MSBELL cross sections for N^{3+} are depicted in Fig. 1c, along with the experimental [36, 39, 41, 42] results and the NXDCB [7], OBO [8], DCBX [41], DWBX [37], BRY [27], and RQIBED [22] calculations. In this case, also, the BRY results underestimate the experimental data. The NXDCB, OBO, DCBX, and DWBX results agree well from threshold to the peak region but slightly underestimate the

experimental results [34, 39] from the peak to the high incident energy region. Here, again, a slight shift in peak position towards the higher energies is observed for the RQIBED results. On the other hand, no such peak position shifting is found for the MSBELL results and hence the present model is successful for the description of EITI cross section data. However, comparisons among the theoretical findings with the experimental cross sections, as shown in Fig. 1a–c, dictate that the MSBELL calculation is the best for the B^+ , C^{2+} , and N^{3+} ions.

Figure 2a–c show the EITI cross sections of beryllium-like O^{4+} , Ne^{6+} , and U^{88+} ions, respectively. The MSBELL predictions for O^{4+} are displayed in Fig. 2a, along with the experimental results [36, 39, 41, 43], and the theoretical DCBX [40], DWBX [37], BRY [27], and RQIBED [22] findings. The predictions from the MSBELL, DCBX, DWBX, and RQIBED theories agree each other but slightly underestimate the experimental results around the peak region. The enhancement in experimental cross sections at around 550 eV is due to the contribution of the EA process [36]. Metastable states of the target particle may also contribute to the enhancement in cross sections. The BRY calculations are lower in magnitude with respect to the experimental cross sections over the wide incident energies except in the high-energy tail.

We present the MSBELL cross sections, along with the experimental results [39, 44, 45], and theoretical findings from DWBARM [6], DCBX [40], RQIBED [22], and BRY [27] for Ne^{6+} , as shown in Fig. 2b. The BRY calculations certainly underestimate the experimental data over almost the whole studied range of incident energies. The MSBELL, DWBARM, and DCBX results provide excellent agreement with each other and also with the experimental data over the energy range considered herein. The RQIBED results are identical in pattern and magnitudes, but slightly shifted in peak position from the peak to the high-energy tail.

The MSBELL predictions for U^{88+} are depicted in Fig. 2c along with the theoretical DWBX [37] and RDWBA [9] findings. To the best of our knowledge, experimental results are not available for U^{88+} . The MSBELL predictions agree well with the DWBX calculations over the domain of incident energies. Hence, the MSBELL predictions, as shown in Fig. 2a–c, provide better success for the description of EITI cross sections for O^{4+} , Ne^{6+} , and U^{88+} targets over the studied incident energies than other theoretical findings considered herein for comparison.

The EITI cross sections for boron-like C^+ , N^{2+} , and O^{3+} targets are depicted in Fig. 3a–c, respectively. The MSBELL predictions for C^+ are displayed in Fig. 3a along with the experimental cross sections [39, 46] and the results of NXDCB [7] and BRY [27] theories. The BRY calculations significantly overestimate the experimental results over the studied range of incident energies. But, the MSBELL predictions

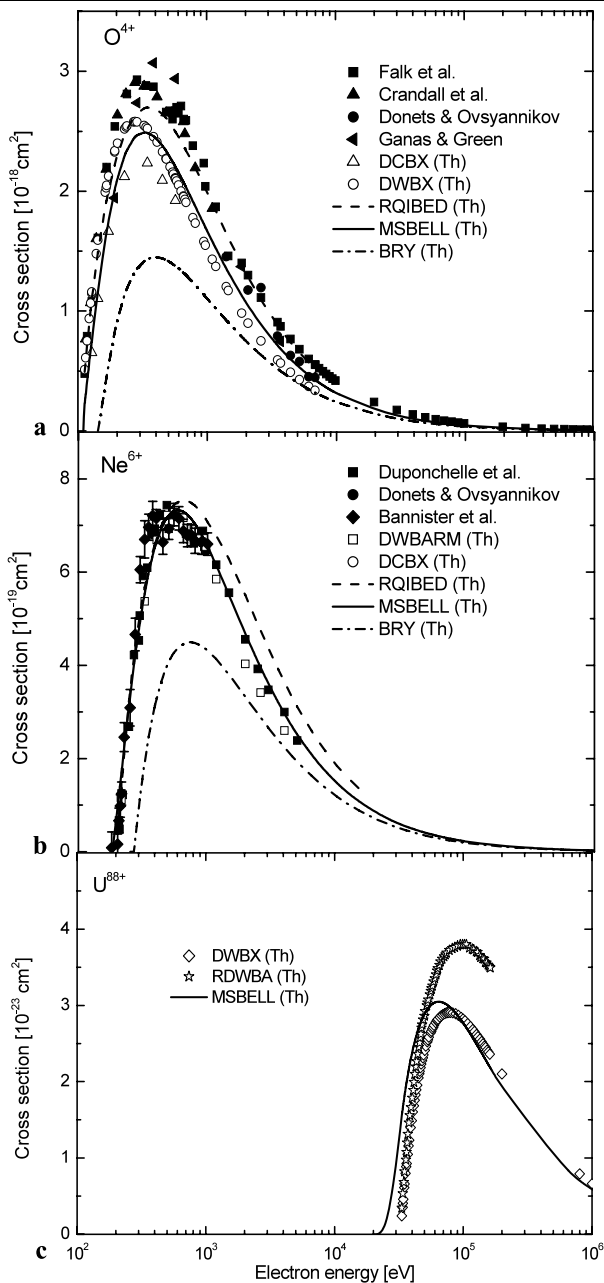


Fig. 2 Same as in Fig. 1 for Be-like ions: (a) O^{4+} , (b) Ne^{6+} , and (c) U^{88+}

exhibit excellent agreement with the NXDCB and experimental data over the whole incident energies.

In Fig. 3b, we present the MSBELL cross sections, experimental results [39, 45, 46], and findings from the NXDCB [7] and BRY [27] theories for N^{2+} . The BRY results largely overestimate in magnitude the experimental results but are identical in pattern with the present calculations. However, as compared to the NXDCB calculations, the MSBELL predictions are successful for the description of experimental EITI cross sections.

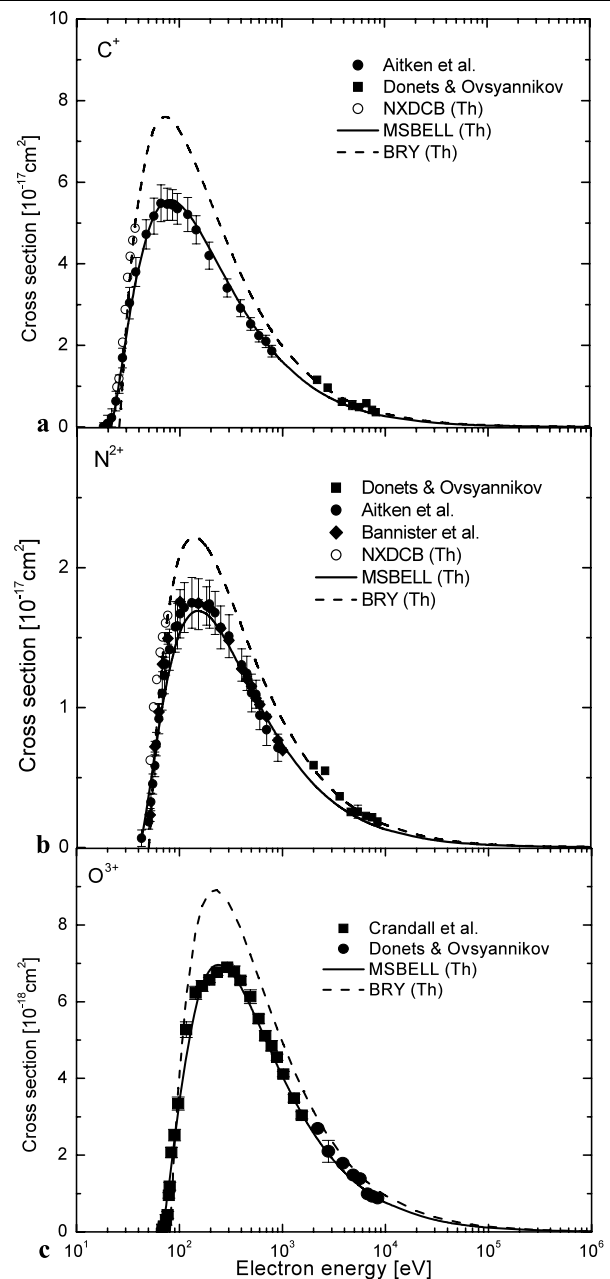


Fig. 3 Same as in Fig. 1 for B-like ions: (a) C^+ , (b) N^{2+} , and (c) O^{3+}

The MSBELL calculations for O^{3+} are depicted in Fig. 3c along with the experimental results [39, 41] and the BRY [27] calculations. The BRY and MSBELL predictions are identical in pattern, but the magnitude of BRY is higher compared to those of experiment. But, excellent agreements are found between the MSBELL and experimental cross sections over the studied range of incident energies. Hence, comparisons among the experimental and theoretical findings, as viewed from Fig. 3a–c, dictate that the predictions from the MSBELL model are the best for the C^+ , N^{2+} , and O^{3+} ionic targets.

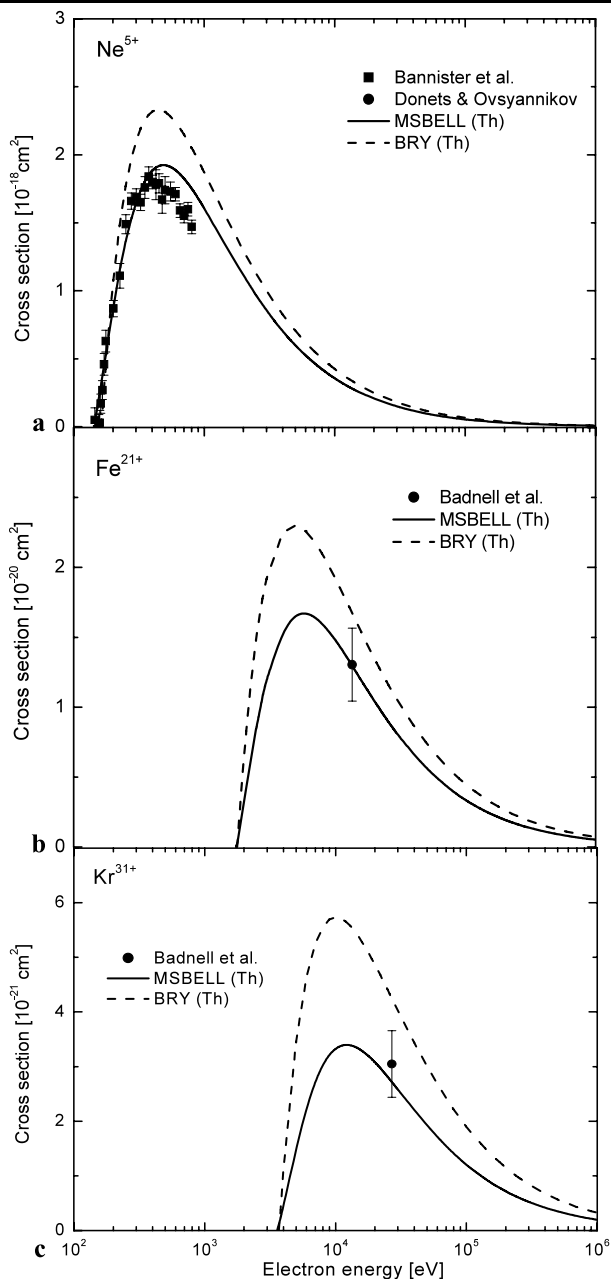


Fig. 4 Same as in Fig. 1 for B-like ions: (a) Ne^{5+} , (b) Fe^{21+} , and (c) Kr^{31+}

Figure 4a–c illustrate the EITI cross sections of boron-like Ne^{5+} , Fe^{21+} , and Kr^{31+} ions, respectively. The MSBELL calculations for Ne^{5+} are displayed in Fig. 4a along with the experimental [39, 45] and BRY [27] cross sections. In this case also the BRY calculations overestimate the experimental cross sections over the domain of incident energies. The MSBELL calculations show identical pattern and agree well with the experimental data except from the peak to 800 eV. This reduction in measured cross sections may occur due to the sources used or to the details of atomic

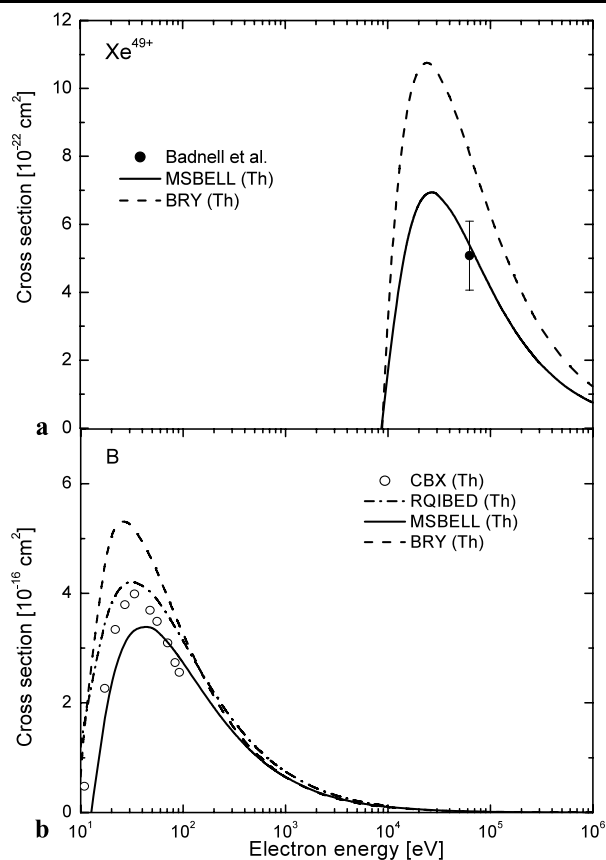


Fig. 5 Same as in Fig. 1 for B-like targets: (a) Xe^{49+} and (b) B

structure and population dynamics for the different species [45].

We present the MSBELL cross sections, experimental results [47], and theoretical findings from BRY [27] for Fe^{21+} in Fig. 4b. Here, again, the BRY calculations are significantly higher in magnitude with respect to the experimental data, but identical with the MSBELL pattern. The present results agree well with the experimental data.

The MSBELL predictions for Kr^{31+} are depicted in Fig. 4c along with the experimental cross sections [47] and theoretical BRY [27] findings. In this case, also, the BRY calculations are remarkably higher in magnitude over the whole incident energy range. But, the MSBELL cross sections agree well with the experimental data within the experimental error. As a whole, the MSBELL predictions produce better agreement for the description of EITI cross sections for the Ne^{5+} , Fe^{21+} , and Kr^{31+} ions over the incident energies considered herein than the available quantum or empirical findings.

Figure 5a and b display the MSBELL calculations for boron-like Xe^{49+} and B. In Fig. 5a, we compare the experimental EITI cross sections [47], along with the findings of the BRY [27] theory, for Xe^{49+} . The MSBELL and BRY cross sections show identical pattern. But, the BRY results significantly misjudge the experimental cross sections.

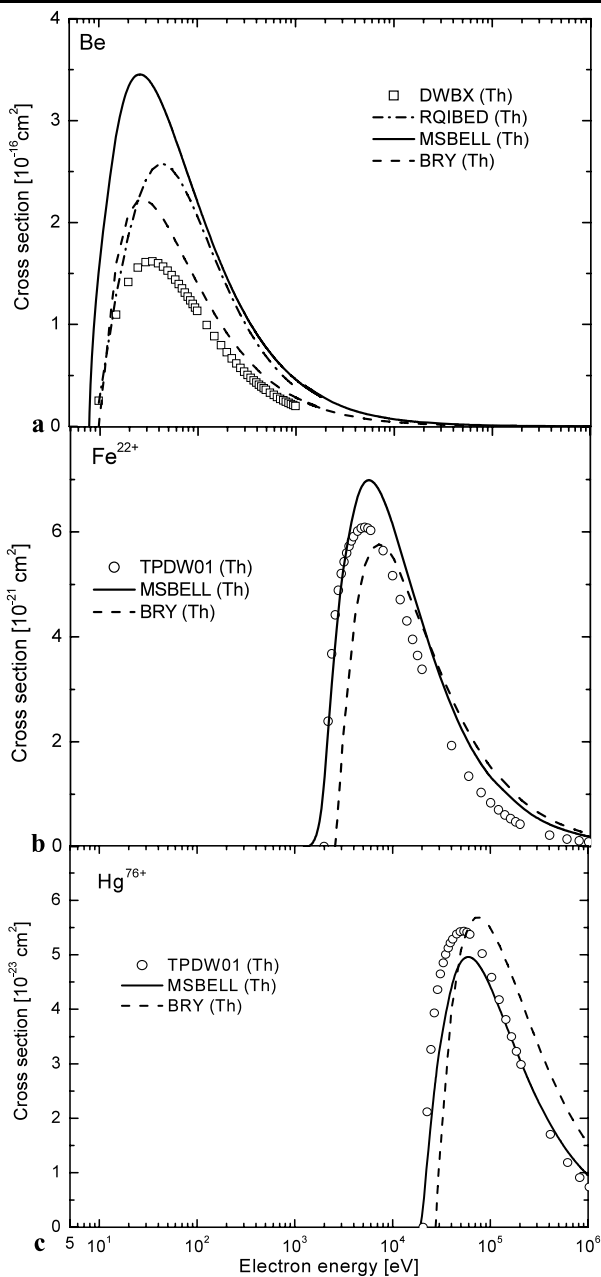


Fig. 6 Same as in Fig. 1 for Be-like targets: (a) Be, (b) Fe^{22+} , and (c) Hg^{76+}

However, the present results produce excellent agreement with the experimental data.

To the best of our knowledge, no experimental data is available for B. Hence, the MSBELL cross sections are depicted in Fig. 5b for B along with the theoretical Coulomb–Born approximation with exchange (CBX [48]), RQIBED [22], and BRY [27] results to adjudge the performance of the present model. No agreements are found among the CBX, RQIBED, and BRY results. But, the MSBELL results agree well with the CBX calculations over the domain of incident energies except in the peak region. Therefore, the MSBELL

model shows better performance, as viewed from Fig. 5a and b, for the description of the EITI experimental data.

As far as we know, experimental results are not available for the beryllium-like Be, Fe^{22+} , and Hg^{76+} targets. The MSBELL predicted EITI cross sections for Be, Fe^{22+} , and Hg^{76+} targets are depicted in Fig. 6a–c to adjudge the results of DWBX [37], RQIBED [22], BRY [27], and TPDW01 (two-potential distorted wave [49]) theories, respectively. No agreements are found among the DWBX, TPDW01, RQIBED, and BRY results. Fair agreements are found between the MSBELL and TPDW01 results. It is interesting to note that interpolation is used to determine the values of the coefficients A_{nl} and B_{nl} for B, Be, Fe^{22+} , and Hg^{76+} targets. Therefore, the MSBELL model may be used for the beryllium- and boron-like targets within the specified range of U_R mentioned in (5) and (6). Finally, the overall performance level of the MSBELL predictions is the best among the other empirical results considered herein for comparison.

4 Conclusions

The MSBELL model, from the overall level of its performance, yields the best success for the description of the experimental EITI cross sections in the beryllium and boron isoelectronic systems with the incident electron energies from threshold to 10^6 eV. As compared to the other theoretical results, the efficiency of the MSBELL model with respect to the domain of species and incident energies considered herein is found the best or better than the other complicated quantum, classical, or empirical methods. It is demonstrated that the MSBELL model provides very encouraging and convincingly accurate results for the Be- and B-like systems. Hence, the MSBELL model with its simple structure may prove to be an efficient alternative for the description of EITI cross sections for the beryllium and boron isoelectronic systems for the applications in the applied sciences and technologies.

References

1. M.R. Talukder, D. Korzec, M. Kando, *J. Appl. Phys.* **91**, 9529 (2002)
2. D. Korzec, M.R. Talukder, M. Kando, *Sci. Technol. Adv. Mater.* **2**, 595 (2001)
3. S. Jones, D.H. Madison, *Phys. Rev. A* **62**, 042701 (2000)
4. J.C. Chang, H.L. Sun, W.Y. Cheng et al., *Phys. Rev. A* **69**, 052713 (2004)
5. S.M. Younger, *Phys. Rev. A* **24**, 1278 (1981)
6. K. Laghdas, R.H.G. Reid, C.J. Joachain et al., *J. Phys. B* **32**, 1439 (1996)
7. D.L. Moores, *J. Phys. B* **11**, L403 (1978)
8. I.E. McCarthy, A.T. Stelbovics, *Phys. Rev. A* **28**, 1322 (1983)
9. D.L. Moores, K.J. Reed, *J. Phys. B* **28**, 4861 (1995)

10. I. Bray, Phys. Rev. A **46**, 6995 (1992)
11. E.J. McGuire, Phys. Rev. A **20**, 445 (1979)
12. K. Butler, D.L. Moores, J. Phys. B **18**, 1247 (1985)
13. H. Jakubowicz, D.L. Moores, J. Phys. B **14**, 3733 (1981)
14. S.M. Younger, Phys. Rev. A **22**, 111 (1980)
15. S.M. Younger, T.D. Märk, in *Electron Impact Ionization*, ed. by T.D. Märk, G.H. Dunn (Springer, Berlin, 1985), p. 24
16. M.S. Gryzinski, Phys. Rev. **138**, 336 (1965)
17. Y.-K. Kim, M.E. Rudd, Phys. Rev. A **50**, 3954 (1994)
18. Y.K. Kim, J.P. Desclaux, Phys. Rev. A **66**, 012708 (2002)
19. H. Deutsch, T.D. Märk, Int. J. Mass Spectrom. Ion Process. **79**, R1 (1987)
20. H. Deutsch, K. Becker, T.D. Märk, Contrib. Plasma Phys. **35**, 421 (1995)
21. H. Deutsch, K. Becker, B. Gstir et al., Int. J. Mass Spectrom. **213**, 5 (2002)
22. M.A. Uddin, A.K.F. Haque, M.S. Mahub et al., Int. J. Mass Spectrom. **244**, 76 (2005)
23. M.A.R. Patoary, M.A. Uddin, A.K.F. Haque et al., Int. J. Quantum Chem. **108**, 1023 (2008)
24. E. Casnati, A. Tartari, C. Baraldi, J. Phys. B **15**, 155 (1982)
25. C. Hombourger, J. Phys. B **31**, 3693 (1998)
26. M.R. Talukder, S. Bose, S. Takamura, Int. J. Mass Spectrom. **269**, 118 (2008)
27. V.A. Bernshtam, Y.V. Ralchenko, Y. Maron, J. Phys. B **33**, 5025 (2000)
28. W. Lotz, Z. Phys. **216**, 241 (1968)
29. W. Lotz, Z. Phys. **232**, 101 (1970)
30. A.L. Godunov, P.B. Ivanov, Phys. Scr. **59**, 277 (1999)
31. K.L. Bell, H.B. Gilbody, J.G. Hughes et al., J. Phys. Chem. Ref. Data **12**, 891 (1983)
32. M.R. Talukder, S. Bose, M.A.R. Patoary et al., Eur. Phys. J. D **46**, 281 (2008)
33. C.J. Fontes, D.H. Sampson, H.L. Zhang, Phys. Rev. A **59**, 1329 (1999)
34. J.P. Desclaux, At. Data Nucl. Data Tables **12**, 325 (1973)
35. M.Y. Amusia, L.V. Chernysheva, *Computations of Atomic Processes* (Institute of Physics, Bristol, 1997)
36. R.A. Falk, G. Stefani, R. Camilloni et al., Phys. Rev. A **28**, 91 (1983)
37. S.M. Younger, J. Quant. Spectrosc. Radiat. Transf. **26**, 329 (1981)
38. P.R. Woodruff, M.-C. Hublet, M.F.A. Harrison, J. Phys. B **11**, 305 (1978)
39. E.D. Donets, V.P. Ovsyannikov, Sov. Phys. JETP **53**, 466 (1981)
40. H. Jakubowicz, D.L. Moores, J. Phys. B **14**, 3733 (1981)
41. D.H. Crandall, R.A. Phaneuf, B.E. Hasselquist et al., J. Phys. B **12**, L249 (1979)
42. D.C. Gregory, D.H. Crandall, R.A. Phaneuf et al., Oak Ridge National Laboratory Rep. ORNL/TM 9501, 1985
43. P.S. Ganas, A.E.S. Grenn, J. Quant. Spectrosc. Radiat. Transfer **25**, 265 (1981)
44. M. Duponchelle, M. Khoulid, E.M. Oualim et al., J. Phys. B **30**, 729 (1997)
45. M.E. Bannister, Phys. Rev. A **5**(4), 1435 (1996)
46. K.L. Aitken, M.F.A. Harrison, R.D. Runder, J. Phys. B **4**, 1189 (1971)
47. N.R. Badnell, M.S. Pindzola, Phys. Rev. A **47**, 2937 (1993)
48. E. Stingl, J. Phys. B **5**, 1160 (1972)
49. T.Y. Kuo, C.J. Chen, S.W. Hsu et al., Phys. Rev. A **48**, 4646 (1993)